medRxiv preprint doi: https://doi.org/10.1101/2020.07.15.20154161; this version posted July 16, 2020. The copyright holder for this preprint (which was not certified by peer review) is the author/funder, who has granted medRxiv a license to display the preprint in perpetuity. It is made available under a CC-BY-NC-ND 4.0 International license .

Projecting the second outbreaks for global COVID-19 pandemic

Jianping Huang[1,*], Xiaoyue Liu[1], Li Zhang[1], Kehu Yang[2], Yaolong Chen[2],
Zhongwei Huang[1], Chuwei Liu[1], Xinbo Lian[1], Danfeng Wang[1]

[1]Collaborative Innovation Center for Western Ecological Safety,
Lanzhou University, Lanzhou, 730000, China.
[2]Evidence-based Medicine Center, Lanzhou University, Lanzhou, 730000, China

* Correspondence author: Jianping Huang (hjp@lzu.edu.cn)

Abstract

COVID-19 is now in an epidemic phase, with a second outbreak likely to appear at any time. The intensity and timing of a second outbreak is a common concern worldwide. In this study, we made scenario projections of the potential second outbreak of COVID-19 using a statistical-epidemiology model, which considers both the impact of seasonal changes in meteorological elements and human social behaviors such as protests and city unblocking. Recent street protests in the United States and other countries are identified as a hidden trigger and amplifier of the second outbreak. The scale and intensity of subsequent COVID-19 outbreaks in the U.S. cities where the epidemic is under initial control are projected to be much greater than those of the first outbreak. For countries without reported protests, lifting the COVID-19 related restrictions prematurely would accelerate the spread of the disease and place mounting pressure on the local medical system that is already overloaded. We anticipate these projections will support public health planning and policymaking by governments and international organizations.

NOTE: This preprint reports new research that has not been certified by peer review and should not be used to guide clinical practice.

medRxiv preprint doi: https://doi.org/10.1101/2020.07.15.20154161; this version posted July 16, 2020. The copyright holder for this preprint (which was not certified by peer review) is the author/funder, who has granted medRxiv a license to display the preprint in perpetuity. It is made available under a CC-BY-NC-ND 4.0 International license .

1 Introduction

Recently, the COVID-19 pandemic has spread rapidly and poses a dire threat to global public health, which claimed over 0.49 million lives, along with 9.8 million confirmed cases as of June 28th [1]. Beyond the spread itself, the outbreak may have far-reaching consequences, negatively affecting the economic development worldwide and posing a series of long-standing social problems[2,3]. There is an urgent need for a global prediction system that can provide scientific guidelines for the World Health Organization and international decision-makers to implement effective containment measures capable of curbing the spread of COVID-19[4]. Researchers worldwide have developed various models with mathematical and statistical methods, including stochastic simulations, lognormal distribution[5], machine learning, and artificial intelligence[6]. Among them, the susceptible-infectious-removed infectious disease model (SIR) is the most widely used[7–9]. However, this simple model is built under a series of idealized assumptions, which may limit the accuracy and reliability of the prediction. In order to obtain the prediction results with higher credibility, more complex models with fewer assumptions should be developed so as to simulate the actual situations in a more realistic manner[10].

Although it is difficult to establish an accurate epidemiological model describing the spread of a pandemic, the reported global pandemic data contain particular solutions to the mathematical equations incorporated in epidemiological models[3,6]. It is theoretically possible to remedy the defects of prior epidemiological models by introducing the latest pandemic data and hence improve the pandemic prediction[2,4,6]. Based on this idea, we have developed a Global Prediction System of the COVID-19 Pandemic (GPCP)[11]. The system develops a modified version of the SIR model and determines the parameters through historical data fitting[12,13], which allows it to make targeted predictions for various countries and obtain better prediction results. The first version of GPCP (CPCP-1) can capture the major features of the daily number of confirmed new cases and provides reliable predictions. However, the prediction of GPCP-1 is only valid for one month[11].

medRxiv preprint doi: https://doi.org/10.1101/2020.07.15.20154161; this version posted July 16, 2020. The copyright holder for this preprint (which was not certified by peer review) is the author/funder, who has granted medRxiv a license to display the preprint in perpetuity. It is made available under a CC-BY-NC-ND 4.0 International license .

In this study, the second version of the Global Prediction System for COVID-19 Pandemic (GPCP-2) is developed based on a modified SEIR model[14]. The system considers both the seasonal changes of meteorological elements and human social behaviors including protests and city unblocking. The paper is arranged as follows: the details of the datasets and the methodology used are given in section 2. In section 3, projections of 12 cities in the United States are presented. The projections of 15 countries with reported protests and 15 countries without reported protests are shown in section 4 and section 5, respectively. Discussion and conclusion are presented in section 6.

2 Method

2.1 The modified SEIR model

The second version of Global Prediction System for COVID-19 Pandemic (GPCP) is built based on a modified SEIR model[15]. The traditional SEIR model[10,14] defines seven states of the disease: susceptible cases (S), insusceptible cases (P), potentially infected cases (E, infected cases in a latent period), infectious cases (I, infected cases that have not been quarantined), quarantined cases (Q, confirmed and quarantined cases), recovered cases (R), and cases of mortality (D). The SEIR model is able to emulate the time curve of an outbreak. The model is consisted of the following equations:

$$dS(t)/dt = -\beta(t)I(t)S(t)/N - \alpha S(t), \quad (1)$$

$$dP(t)/dt = \alpha S(t), \quad (2)$$

$$dE(t)/dt = \beta(t)I(t)S(t)/N - \gamma(t)E(t), \quad (3)$$

$$dI(t)/dt = \gamma(t)E(t) - \delta(t)I(t), \quad (4)$$

$$dQ(t)/dt = \delta(t)I(t) - \lambda(t)Q(t) - \kappa(t)Q(t) \quad (5)$$

$$dR(t)/dt = \lambda(t)Q(t) \quad (6)$$

$$dD(t)/dt = \kappa(t)Q(t) \quad (7)$$

The sum of the six categories is equal to the total population (N) at any time.

$$S + P + E + I + Q + R + D = N$$

We modified the model by introducing the timing of community reopening collected from

medRxiv preprint doi: https://doi.org/10.1101/2020.07.15.20154161; this version posted July 16, 2020. The copyright holder for this preprint (which was not certified by peer review) is the author/funder, who has granted medRxiv a license to display the preprint in perpetuity. It is made available under a CC-BY-NC-ND 4.0 International license .

news reports. If the timing collected from news reports is not explicit enough as an input to our model, the timing will be indicated by the daily new cases on the day of reopening (dQ_c). As the number of newly confirmed cases on a given day falls lower than dQ_c, local authority begins to lift or loose the lockdowns.

In addition, the temporal variation of transmission rate due to changes in local temperature as well as human behaviors are considered. Generally, the transmission rate ($\beta(t)$) can be expressed by the following equations:

$$\beta(t) = \begin{cases} \beta_0 & t < t_{int} \\ \beta_1 & t_{int} \leq t < t_{lift} \\ \beta_2 + E \times F(t) & t \geq t_{lift} \end{cases}$$

where β_0 represents the transmission rate in the non-intervention period at the early stage of the pandemic ($t < t_{int}$); β_1 represents the transmission rate during the intervention period ($t_{int} \leq t < t_{lift}$); β_2 represents the transmission rate after the restriction is lifted. β_0 and β_1 are fitted against the actual reported data, while β_2 is the assumed value in possible future scenarios. We assume a 14-day delay in the effect of the intervention on the infection rate. $F(t)$ is the PDF function obtained by Huang et al.[16], who found that 60.0% of confirmed COVID-19 cases occurred in places where the air temperature ranged from 5°C to 15°C. Using the NCEP reanalysis data, we calculated the global distribution of probability distribution function (PDF) values on each day of the year and included its influence on the infection rate. Figure 1 shows the PDF values for the four seasons in a year. High PDF values correspond to the ambient temperature that is conducive for the virus to spread. For the northern hemisphere, the optimal band generally moves northward in summer (June, July, and August) and moves southward in winter (December, January, and February), while for southern hemisphere the optimal band moves southward in summer (December, January, and February) and moves northward in winter (June, July, and August).

medRxiv preprint doi: https://doi.org/10.1101/2020.07.15.20154161; this version posted July 16, 2020. The copyright holder for this preprint (which was not certified by peer review) is the author/funder, who has granted medRxiv a license to display the preprint in perpetuity. It is made available under a CC-BY-NC-ND 4.0 International license .

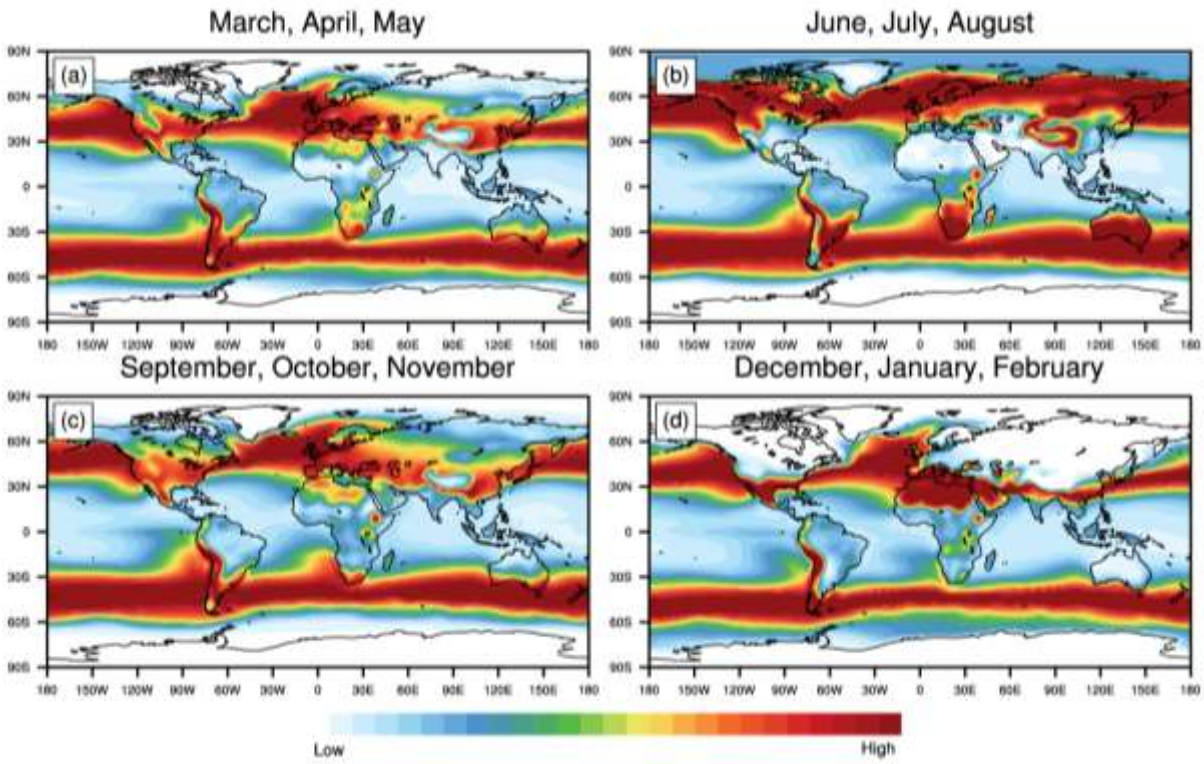

Figure 1: The optimal temperature zone for the spread COVID-19. Regions with warm shadings indicate more conducive temperature for the spread of the virus and vice versa.

Since the seasonality of transmission is still disputed and future trajectory of the outbreaks may be influenced by the intensity of intervention measures, four future scenarios are designed to project the epidemic after easing COVID-19 related restrictions:

- **Scenario 1**: The restrictions are completely lifted after t_{int} $(\beta_2 = \beta_0)$. The seasonal forcing on the transmission rate is considered (E = 1).
- **Scenario 2**: The restrictions are partially lifted after t_{int} $(\beta_2 = (\beta_0 + \beta_1)/2)$. The seasonal forcing on the transmission rate is considered (E = 1).
- **Scenario 3**: The restrictions are completely lifted after t_{int} $(\beta_2 = \beta_0)$. The seasonal forcing on the transmission rate is not considered (E = 0).
- **Scenario 4**: The restrictions are partially lifted after t_{int} $(\beta_2 = (\beta_0 + \beta_1)/2)$. The seasonal forcing on the transmission rate is not considered (E = 0).

2.2 Parameter fitting and numerical solutions

In order to enhance the stability of the traditional least square method (Gauss-Newton algorithm), we use an improved damped least square method called Levenberg-Marquardt

medRxiv preprint doi: https://doi.org/10.1101/2020.07.15.20154161; this version posted July 16, 2020. The copyright holder for this preprint (which was not certified by peer review) is the author/funder, who has granted medRxiv a license to display the preprint in perpetuity. It is made available under a CC-BY-NC-ND 4.0 International license .

algorithm[17]. This method inserts a damping coefficient into the Gauss-Newton method when calculating the Hessian matrix. The benefit of introducing this damping coefficient is that it can converge very quickly in the steepest direction in many cases even when the initial solution is very far from ideal values, which makes the parameter determination more robust[18]. In addition, for all damping coefficient greater than 0, the coefficient matrix is positive definite which makes the Hessian matrix in the descending direction. The input variables to obtain fitted parameters ($\alpha, \beta, \gamma, \delta, \lambda,$ and κ) are the time series of confirmed ($Q(t) - D(t) - R(t)$), death ($D(t)$), and recovered ($R(t)$) cases provided by from Johns Hopkins University Center for Systems Science and Engineering[1]. The equations are solved using the classic 4th order Runge-Kutta method.

3 Projections of the US cities

Unfortunately, the recent protests against police violence in cities across the United States have gone ahead despite the current rising COVID-19 pandemic and potential subsequent outbreaks, possibly with higher intensity. Large public gatherings, shouting, and marching shoulder to shoulder may have already sown the seeds of the second outbreaks in regions under initial control[19,20] and made it even more difficult to contain the epidemic in regions where the curve is still increasing. The use of tear gas and pepper spray against the protesters may also have produced violent coughing and runny noses, forcing protesters to remove their masks and making the crowds even more susceptible to the virus. A certain number of patients with the latent disease may have participated in the protests and spread the disease to healthy protesters, police officers, and national guards who are not yet immune to the virus[21]. If the close contacts of the infectious are not fully tracked, they may spread the virus to other groups of people, increasing the risk of a larger size of outbreaks. Here, we simulated the impact of large-scale protests on the potential second outbreaks in several cities of the United States[22] (Figure 2 and Table 1). The model generally predicted a second wave of COVID-19 in the second half of 2020. We estimated the increase in the population of potentially infected people (δE_t) for each city based on the ratio of the number of infected persons (Q_t) to the total population of the city

medRxiv preprint doi: https://doi.org/10.1101/2020.07.15.20154161; this version posted July 16, 2020. The copyright holder for this preprint (which was not certified by peer review) is the author/funder, who has granted medRxiv a license to display the preprint in perpetuity. It is made available under a CC-BY-NC-ND 4.0 International license .

(N). The timing of protests and the number of protesters in each city were collected from local news reports (Table 1). The increase in the population of potentially infected people (δE_t) and the populations of protesters (δS_t, regarded as an increase in the population of susceptible) were used as the force input for the model calculations to simulate the impact of protests on the outbreaks. When the protests begin, we force group E and group S to increase δE_t and δS_t, respectively.

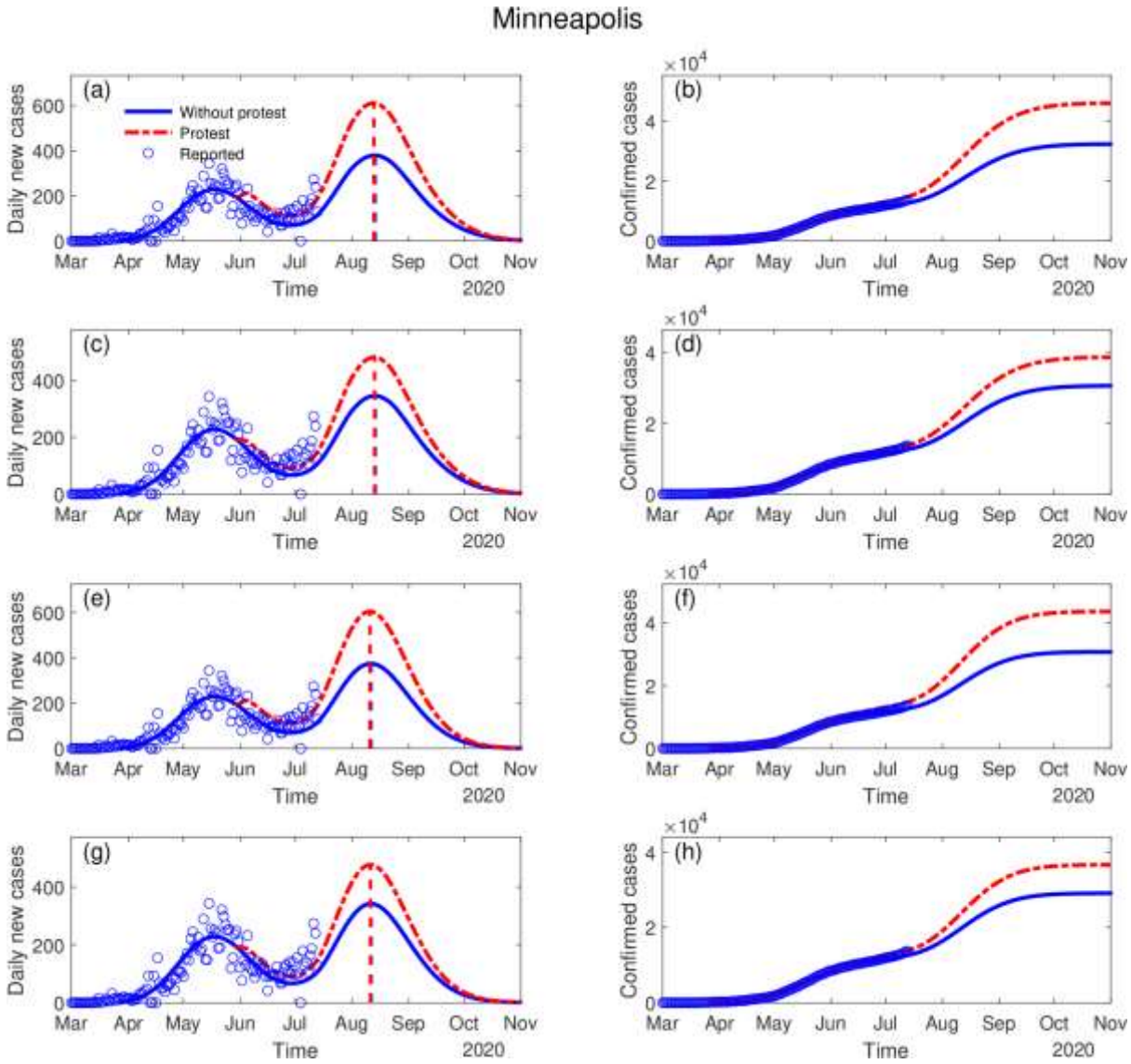

Figure 2: The impact of protests on the possible second outbreak in Minneapolis. The blue dots denote the reported daily incidence of COVID-19 cases. The blue line represents the simulation and projections without protests, while the dashed red line denotes the simulation and projections with protests. Four scenarios with protests and four scenarios without protests are simulated. (a)~ (b), (c)~(d), (e)~(f), (g)~(h) are the simulation for Scenario 1, 2, 3, 4,

medRxiv preprint doi: https://doi.org/10.1101/2020.07.15.20154161; this version posted July 16, 2020. The copyright holder for this preprint (which was not certified by peer review) is the author/funder, who has granted medRxiv a license to display the preprint in perpetuity. It is made available under a CC-BY-NC-ND 4.0 International license .

respectively. (a)~(b) and (c)~(d) are the simulations with seasonal forcing; (e)~(f) and (g)~(h) are the simulations without seasonal forcing. (a)~(b) and (e)~(f) are the simulations where the restrictions are completely lifted; (c)~(d) and (g)~(h) are the simulations where the restrictions are partially lifted.

Figure 2 shows the projections for Minneapolis in 8 scenarios (4 scenarios with protests and 4 without). After the COVID-19 restrictions were lifted, an upward trend of daily new cases has been observed. The protests would significantly amplify the intensity of the second outbreak but may not be able to advance it. In scenarios 1, the second outbreak of Minneapolis will peak in mid-August 2020. The comparison between scenarios indicates that the effect of intervention measures outweighs the seasonal forcing. For the rest of the 12 cities, the model also predicted enhanced second outbreaks when the impact of protests is considered (Table 1). Due to space constraints, the details of the projection results are not presented in the manuscript and can be accessed at http://covid-19.lzu.edu.cn/.

Table 1 Projections of the second outbreaks in some US cities in Scenario 1

Countries	Population (million)	Start date of Protests	Estimated participants	The peak time of the second outbreaks	Peak time daily new incidence without protests	Peak time daily new incidence with protests	End of the second outbreak	Accumulated Confirmed Cases
New York City (New York)	8.33	May, 29th	25,000	Mid-August	Around 8,000	Around 18,000	End of 2020	Around 900,000
Chicago (Illinois)	5.15	May, 28th	30,000	Mid-September	Around 2700	Around 4100	End of 2020	Around 390,000
Minneapolis (Minnesota)	1.26	May, 26th	30,000	Mid-September	Around 400	Around 700	End of 2020	Around 48,000
Columbus (Ohio)	1.31	May, 28th	10,000	Late-September	Around 120	Around 380	End of 2020	Around 35,000
Westchester (Illinois)	0.97	May, 29th	30,000	Mid-August	Around 3,500	Around 5,500	September, 2020	Around 150,000
Philadelphia (Pennsylvania)	10.04	May, 30th	10,000	Mid-October	Around 800	Around 1,700	End of 2020	Around 120,000
Seattle (Washington)	2.25	May, 29th	50,000	Late-August	Around 2,00	Around 600	End of 2020	Around 35,000
Washington, D.C.	0.70	May, 29th	10,000	Mid-October	Around 180	Around 650	September, 2020	Around 70,000
San Francisco (California)	0.88	May, 30th	30,000	Mid-August	Around 100	Around 400	October, 2020	Around 22,000
Detroit (Michigan)	1.75	May, 29th	30,000	Early-September	Around 1,000	Around 2,200	October, 2020	Around 70,000
Miami-Dade (Florida)	2.72	May, 30th	20,000	Mid-August	Around 1,800	Around 3,000	September, 2020	Around 120,000
San Diego (California)	3.34	May, 29th	30,000	Late-August	Around 1,000	Around 1,600	September, 2020	Around 130,000

medRxiv preprint doi: https://doi.org/10.1101/2020.07.15.20154161; this version posted July 16, 2020. The copyright holder for this preprint (which was not certified by peer review) is the author/funder, who has granted medRxiv a license to display the preprint in perpetuity. It is made available under a CC-BY-NC-ND 4.0 International license .

4 Projections of countries with reported protests

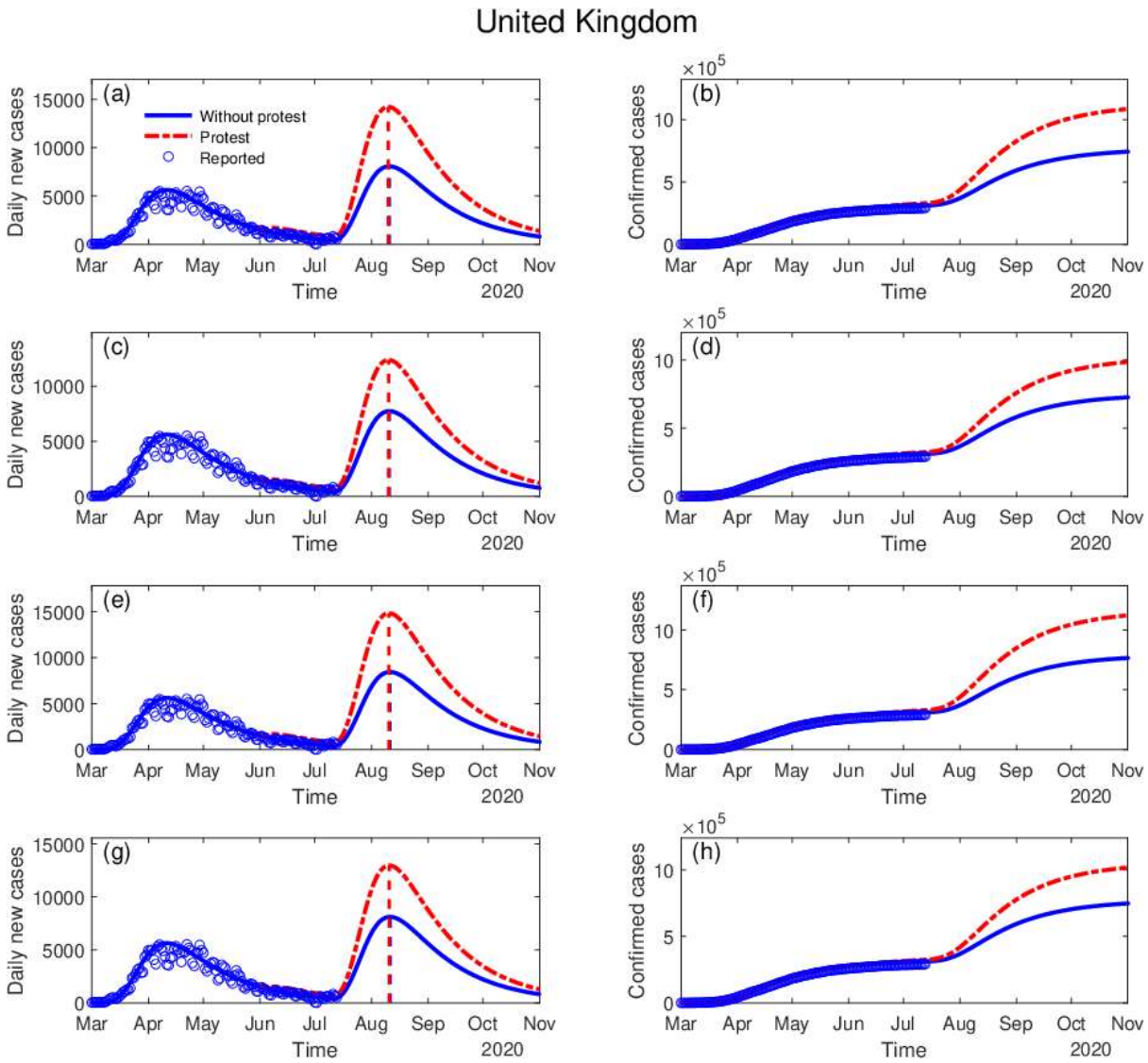

Figure 3: The impact of protests on the possible second outbreak in the United Kingdom. The blue dots denote the reported daily incidence of COVID-19 cases. The blue line represents the simulation and projections without protests, while the dashed red line denotes the simulation and projections with protests. The scenarios in these subplots are the same as Figure 2.

In addition to the United States, protests of a certain scale also broke out in other countries. Using similar parameterization of the protests, Table 3 presents the projections of the second outbreaks in the United Kingdom, the United States, Germany, Italy, Australia, Canada, Spain, Mexico, Switzerland, Belgium, Netherlands, Ireland, and Denmark. For the United Kingdom (Figure 3), the second outbreak is likely to peak during August. Under the impact of protests,

medRxiv preprint doi: https://doi.org/10.1101/2020.07.15.20154161; this version posted July 16, 2020. The copyright holder for this preprint (which was not certified by peer review) is the author/funder, who has granted medRxiv a license to display the preprint in perpetuity. It is made available under a CC-BY-NC-ND 4.0 International license .

when the restrictions are lifted completely, a second wave with a peak of 14,160 is expected, which is 75.6% higher than the scenario without protests (Scenario 1). The protests and the lifting of restrictions, along with the enhancement in the ability of virus transmission in the cold seasons due to temperature change may cause the recurrence of an outbreak that was initially under control. If the same intervention measures are implemented during the second outbreak, the second outbreak would be brought under control again by the end of 2020.

Table 2 Projections of the second outbreaks in some countries (with protests)

Countries	Population (million)	Start date of Protests	Estimated participants	The peak time of the second outbreaks	Peak time daily new incidence without protests	Peak time daily new incidence with protests	End of the second outbreak	Accumulated Confirmed Cases with protests
United Kingdom	66.48	May, 28th	70,000	Early-August	Around 8,000	Around 14,170	End of 2020	Around 1,150,000
United States	328.2	May, 26th	1,500,000	Late-July	Around 40,000	Around 120,000	End of 2020	Around 16,000,000
Germany	82.93	May 30th	160,000	Early-September	Around 4,500	Around 7,000	End of 2020	Around 450,000
Italy	60.43	June, 30th	150,000	Early-October	Around 6,000	Around 95,000	End of 2020	Around 600,000
Australia	25.44	June, 2nd	14,000	Early-August	Around 500	Around 1,900	End of 2020	Around 45,000
Canada	37.05	May, 30th	100,000	Late-September	Around 1,800	Around 2,500	End of 2020	Around 250,000
Spain	46.73	June, 1st	10,000	Early-September	Around 7,600	Around 9,400	End of 2020	Around 1,100,000
Mexico	126.2	May, 30th	50,000	Late-August	Around 5,800	Around 7,600	End of 2021	Around 1,500,000
Switzerland	8.57	May, 31st	20,000	Early-August	Around 1,400	Around 2,100	October, 2020	Around 80,000
Belgium	11.42	June, 1st	50,000	Late-August	Around 2,000	Around 4,200	End of 2020	Around 230,000
Netherlands	17.26	June, 1st	56,000	Late-July	Around 1,800	Around 2,800	End of 2020	Around 170,000
Ireland	4.81	May, 31st	20,000	Mid-July	Around 600	Around 1,500	End of 2020	Around 90,000
Denmark	5.73	May 31st	20,000	Late-August	Around 600	Around 1,000	End of 2020	Around 60,000

medRxiv preprint doi: https://doi.org/10.1101/2020.07.15.20154161; this version posted July 16, 2020. The copyright holder for this preprint (which was not certified by peer review) is the author/funder, who has granted medRxiv a license to display the preprint in perpetuity. It is made available under a CC-BY-NC-ND 4.0 International license .

5 Projections of countries without reported protest

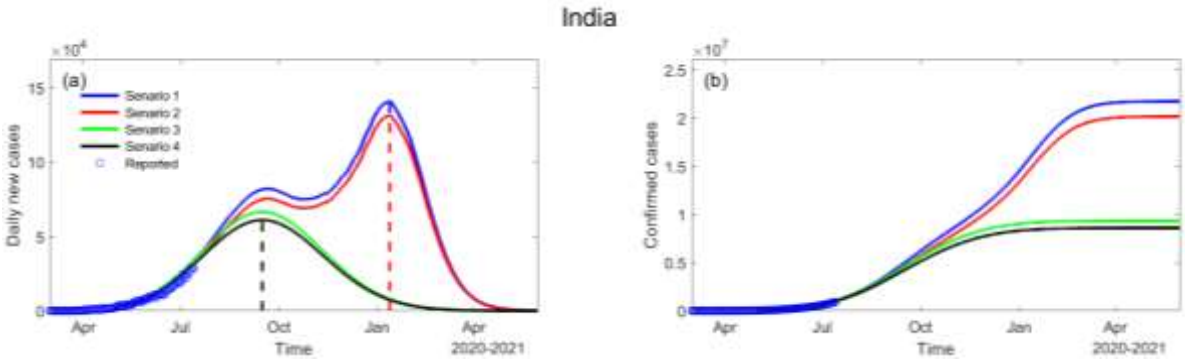

Figure 4: Projections of the second outbreak in India in different scenarios. Scenarios 1 and 2 are simulated with seasonal forcing, while scenarios 3 and 4 are simulated without seasonal forcing. Scenarios 1 and 3 are the projections where restrictions are fully lifted, while scenarios 2 and 4 are the projections where restrictions are partially lifted.

Mass gathering events during the epidemic should be restricted or even banned since they have the potential to enhance the second outbreak and pose further radical public-health challenges for health authorities and governments[23,24]. Lifting the restrictions too early may also have the potential to trigger subsequent outbreaks and further increase the pressure on the medical system. Fig 4 shows the projections of India in the four scenarios. With seasonal forcing, it is predicted that the first peak of the epidemic will occur in September while the second peak with higher intensity, caused environmental changes, will arrive in January 2021. Without seasonal forcing, there would be only one peak in September 2020. We also projected the epidemic curve for other countries including Russia, Brazil, Chile, etc. that are still in the rapid growing period. We classified them as 'non-protesting countries', not because there are no protests. Indeed, there might have been many protests and mass gatherings in India, Brazil, and other regions that may impact the outbreak on varying degrees, but the information on the timing and size of these protests are currently not available. Therefore, the role of these protests on the timing and size of the outbreaks can not be isolated and may not be incorporated as a force into the model.

From Table 3 we can see that the peak time and size of the second outbreak varies from countries to countries, due to different levels of interventions measures, environmental

medRxiv preprint doi: https://doi.org/10.1101/2020.07.15.20154161; this version posted July 16, 2020. The copyright holder for this preprint (which was not certified by peer review) is the author/funder, who has granted medRxiv a license to display the preprint in perpetuity. It is made available under a CC-BY-NC-ND 4.0 International license .

conditions, medical resources, etc. Regions with high population density are at higher risk of enhanced second outbreaks. When control measures are lifted too soon and environmental temperatures are more suitable for the spread of disease[25], an enhanced second outbreak is expected. Therefore, when considering the timing of lifting the restrictions to restore the economy, it is necessary to analyze epidemic situations as well as climate factors. For example, during cold seasons when the transmission rate is higher, reopening would easily light up the second outbreaks, since conducive environmental factors and related human social behaviors (more frequent indoor gatherings) would, directly and indirectly, increase the transmission ability of the virus, leaving more people vulnerable to infection. Therefore, the peak of the second wave of the outbreak is most likely to synchronize with the fall of environmental temperature, displaying strong seasonality. During winter months, the temperate regions of the Northern and Southern Hemispheres experience highly synchronized annual influenza epidemics[26]. Additionally, when restrictions are lifted, personal protection (wearing face masks, keeping appropriate interpersonal distance, sterilization, etc)[27]. is still required or even mandatory in indoor places so as to minimize the infection rate by cutting off the infection routine.

Table 3 Projections of the second outbreaks in some countries in Scenario 1 (without reported protests)

Countries	Population (million)	The peak time of the second outbreaks	Peak time daily new incidence without protests	End of the second outbreak	Accumulated Confirmed Cases
India	1324	Early-November, 2020	Around 41,000	February, 2021	Around 6,000,000
Russia	144.5	Late-September, 2020	Around 12,000	April, 2021	Around 2,800,000
Brazil	209.5	Early-October, 2020	Around 60,000	February, 2021	Around 11,200,000
Peru	32.05	Late-October, 2020	Around 13,000	May, 2021	Around 2,500,000
Chile	18.60	Late-July, 2020	Around 11,000	April, 2021	Around 1,500,000
Argentina	44.49	January, 2021	Around 5000	April, 2021	Around 600,000
Pakistan	212.2	Early-August, 2020	Around 30,000	November, 2020	Around 2,700,000
Saudi Arabia	32.55	Late-July, 2020	Around 13,000	May, 2021	Around 3,500,000
Bangladesh	161.4	Late-August, 2020	Around 15,000	January, 2021	Around 1,600,000
Qatar	2.64	Early-September, 2020	Around 2,400	December, 2020	Around 240,000
Colombia	49.64	February, 2021	Around 12,500	May, 2021	Around 55,000
Belarus	9.51	Mid-August, 2020	Around 2,800	May, 2021	Around 2,800,000
Egypt	102.27	Mid-November, 2020	Around 2,800	March, 2021	Around 420,000
Ecuador	17.08	Mid-August, 2020	Around 5,000	December, 2020	Around 300,000

medRxiv preprint doi: https://doi.org/10.1101/2020.07.15.20154161; this version posted July 16, 2020. The copyright holder for this preprint (which was not certified by peer review) is the author/funder, who has granted medRxiv a license to display the preprint in perpetuity. It is made available under a CC-BY-NC-ND 4.0 International license .

6 Discussion and conclusion

New treatments and vaccines are not yet available for any COVID-19-affected areas[28]. With the presence asymptomatic of carriers that may spread the virus, and the lack of herd immunity, a second outbreak is inevitable as confirmed cases of COVID-19 increase. Our results show that the timing and intensity of the second outbreaks are seasonally modulated and depend largely on local reopening policies. Higher seasonal variations in COVID-19 transmission may lead to a greater incidence of recurrent wintertime outbreaks[29]. The current mass protests in the United States and other regions of the world could lead to amplified second outbreaks, overlapping the wintertime outbreaks and threatening more lives. This is because the extremely crowded environments facilitate the spread of the virus, leading to high rates of the second attack, as seen in both the 1918 pandemic and the 1957 Asian influenza pandemic[30–32].

If the transmission capacity of the second outbreak increases, it could place a catastrophic burden on the health system and create even more serious social and economic crises. However, if the chain of transmission is cut during the first outbreak, there will be no further outbreak similar to the first wave. The necessary drug therapies and vaccines currently require long-term development and testing, so nonpharmaceutical interventions are the only direct means available to suppress the spread of the disease[33]. In the face of a powerful pandemic, everyone must help to fight the virus. We must collectively follow the distancing limits recommended by global public-health organizations to effectively reduce the potential cost in the lives of the second wave of infection. Our findings should encourage close monitoring and early warning of the development of a global pandemic, as well as safeguards for our global prediction system to best contain the second wave[34]. These results provide a powerful scientific basis for governments to adjust their policies and control measures in real-time, to achieve the most effective allocation of medical resources before the second outbreak and to reduce the associated health risks.

medRxiv preprint doi: https://doi.org/10.1101/2020.07.15.20154161; this version posted July 16, 2020. The copyright holder for this preprint (which was not certified by peer review) is the author/funder, who has granted medRxiv a license to display the preprint in perpetuity. It is made available under a CC-BY-NC-ND 4.0 International license .

Acknowledgments: The authors acknowledge the Center for Systems Science and Engineering (CSSE) at Johns Hopkins University for providing the COVID-19 data. We acknowledge E. Cheynet for providing the Generalized SEIR Epidemic Model (fitting and computation). This work was jointly supported by the National Science Foundation of China (41521004) and the Gansu Provincial Special Fund Project for Guiding Scientific and Technological Innovation and Development (Grant No. 2019ZX-06).

References

1. COVID-19 Data repository by the Center for Systems Science and Engineering (CSSE) at Johns Hopkins University 2020. https://github.com/CSSEGISandData/COVID-19.

2. Nicola, M. *et al.* The socio-economic implications of the coronavirus pandemic (COVID-19): a review. *Int. J. Surg.* **78**, 185–193 (2020).

3. World Health Organization (WHO). Coronavirus disease 2019 situation report 51 11th March 2020. *World Heal. Organ.* **2019**, 2633 (2020).

4. Petropoulos, F. & Makridakis, S. Forecasting the novel coronavirus COVID-19. *PLoS One* **15**, 1–8 (2020).

5. Linton, N. M. *et al.* Incubation period and other epidemiological characteristics of 2019 novel coronavirus infections with right truncation: a statistical analysis of publicly available case data. *J. Clin. Med.* **9**, 538 (2020).

6. Tuli, S., Tuli, S., Tuli, R. & Gill, S. S. Predicting the growth and trend of COVID-19 pandemic using machine learning and cloud computing. *Internet of Things* (2020) doi:10.1016/j.iot.2020.100222.

7. Wu, J. T., Leung, K. & Leung, G. M. Nowcasting and forecasting the potential domestic and international spread of the 2019-nCoV outbreak originating in Wuhan,

medRxiv preprint doi: https://doi.org/10.1101/2020.07.15.20154161; this version posted July 16, 2020. The copyright holder for this preprint (which was not certified by peer review) is the author/funder, who has granted medRxiv a license to display the preprint in perpetuity. It is made available under a CC-BY-NC-ND 4.0 International license .

China: a modelling study. *Lancet* **395**, 689–697 (2020).

8. Wang, H. *et al.* Phase-adjusted estimation of the number of coronavirus disease 2019 cases in Wuhan, China. *Cell Discov.* **6**, 10 (2020).

9. Yang, Z. *et al.* Modified SEIR and AI prediction of the epidemics trend of COVID-19 in China under public health interventions. *J. Thorac. Dis.* (2020) doi:10.21037/jtd.2020.02.64.

10. Godio, A., Pace, F. & Vergnano, A. SEIR Modeling of the Italian Epidemic of SARS-CoV-2 Using Computational Swarm Intelligence. *Int. J. Environ. Res. Public Health* **17**, 3535 (2020).

11. Huang, J. *et al.* Global prediction system for COVID-19 pandemic. *Sci. Bull.* (2020).

12. Huang J. and Y. Yi., Inversion of nonlinear dynamical model from the observation. Science in China (B). 34, 1246-1251 (1991).

13. Huang J., Y. Yi, S. Wang, and J. Chou. 1993: An analogue-dynamical long-range numerical weather prediction system incorporating historical evolution. Quarterly Journal of the Royal Meteorological Society. 119, 547-565 (1993). DOI: 10.1002/qj.49711951111.

14. Peng, L., Yang, W., Zhang, D., Zhuge, C. & Hong, L. Epidemic analysis of COVID-19 in China by dynamical modeling. *medRxiv* 1–18 (2020) doi:https://doi.org/10.1101/2020.02.16.20023465.

15. Cheynet, E. Generalized SEIR epidemic model (fitting and computation). *Github* (2020).

16. Huang, Z. *et al.* Optimal temperature zone for the dispersal of COVID-19. *Sci. Total Environ.* 139487 (2020) doi:10.1016/j.scitotenv.2020.139487.

17. Madsen, K., Nielsen, H. B. & Tingleff, O. *Methods for non-linear least squares problems.* (2004). doi:10.1155/2012/312985.

medRxiv preprint doi: https://doi.org/10.1101/2020.07.15.20154161; this version posted July 16, 2020. The copyright holder for this preprint (which was not certified by peer review) is the author/funder, who has granted medRxiv a license to display the preprint in perpetuity. It is made available under a CC-BY-NC-ND 4.0 International license .

18. Kőházi-Kis, A. Relative effectiveness of the trust-region algorithm with precise secund order derivatives. **6**, 1–7 (2019).

19. Kim, C. Images of police using violence against peaceful protesters are going viral. https://www.vox.com/2020/5/31/21275994/police-violence-peaceful-protesters-images.

20. Rothenberg, C., Achanta, S., Svendsen, E. R. & Jordt, S. E. Tear gas: an epidemiological and mechanistic reassessment. *Ann. N. Y. Acad. Sci.* **1378**, 96–107 (2016).

21. Parodi, S. M. & Liu, V. X. From containment to mitigation of COVID-19 in the US. *JAMA - J. Am. Med. Assoc.* **323**, 1441–1442 (2020).

22. Rocklöv, J. & Sjödin, H. High population densities catalyse the spread of COVID-19. *J. Travel Med.* **27**, 1–2 (2020).

23. McCloskey, B. *et al.* Mass gathering events and reducing further global spread of COVID-19: a political and public health dilemma. *The Lancet* vol. 395 1096–1099 (2020).

24. Petersen, E. *et al.* Rapid spread of zika virus in the Americas - implications for public ealth preparedness for mass gatherings at the 2016 Brazil Olympic Games. *International Journal of Infectious Diseases* vol. 44 11–15 (2016).

25. Tosepu, R. *et al.* Correlation between weather and COVID-19 pandemic in Jakarta, Indonesia. *Sci. Total Environ.* **725**, (2020).

26. Tamerius, J. D. *et al.* Environmental predictors of seasonal influenza epidemics across temperate and tropical climates. *PLoS Pathog.* (2013) doi:10.1371/journal.ppat.1003194.

27. World Health Organization(WHO). Coronavirus disease (COVID-19) advice for the public. https://www.who.int/emergencies/diseases/novel-coronavirus-2019/advice-for-

medRxiv preprint doi: https://doi.org/10.1101/2020.07.15.20154161; this version posted July 16, 2020. The copyright holder for this preprint (which was not certified by peer review) is the author/funder, who has granted medRxiv a license to display the preprint in perpetuity. It is made available under a CC-BY-NC-ND 4.0 International license .

public.

28. Bai, Z. *et al.* The rapid assessment and early warning models for COVID-19. *Virologica Sinica* (2020) doi:10.1007/s12250-020-00219-0.

29. Kissler, S. M., Tedijanto, C., Goldstein, E., Grad, Y. H. & Lipsitch, M. Projecting the transmission dynamics of SARS-CoV-2 through the postpandemic period. *Science* (2020) doi:10.1126/science.abb5793.

30. Rainey, J. J., Phelps, T. & Shi, J. Mass gatherings and respiratory disease outbreaks in the United States – should we be worried? results from a systematic literature review and analysis of the national outbreak reporting system. *PLoS One* **11**, e0160378 (2016).

31. Tomes, N. 'Destroyer and teacher': managing the masses during the 1918-1919 influenza pandemic. *Public Health Reports* vol. 125 48–62 (2010).

32. Alexander Langmuir, M. D. Asian influenza in the United States. *Ann. Intern. Med.* **49**, 483 (1958).

33. Prem, K. *et al.* The effect of control strategies to reduce social mixing on outcomes of the COVID-19 epidemic in Wuhan, China: a modelling study. *Lancet Public Heal.* **5**, e261–e270 (2020).

34. Shea, K. *et al.* Harnessing multiple models for outbreak management. *Science* (2020) doi:10.1126/science.abb9934.